

# Multi-Object, Near-IR Grism Spectroscopy with the 6.5m MMT

Rose A. Finn, Donald W. McCarthy

Steward Observatory, 933 N. Cherry Ave, Tucson, AZ 85721

## ABSTRACT

Wide-field infrared cameras, operating on the new generation of large telescopes, offer unprecedented gains in the detection of faint sources and in observing efficiency for both direct imaging and spectroscopy. PISCES, a near-IR (1-2.5 micron) wide-field camera designed for the f/9 secondaries of the Steward 2.3m and 6.5m MMT, is one such instrument that has been operational for over one year. Equipped with a 1024x1024 HAWAII HgCdTe array, PISCES offers an 8.5 arcminute field at the 2.3m and a 3.1 arcminute field at the MMT. Here we present our design to upgrade PISCES with a low resolution ( $R=200-500$ ) grism for single and multi-object spectroscopy. The design allows J, H, and K-band spectroscopy in orders 5, 4 and 3, respectively. The combination of 6.5m aperture and multi-object capability will make PISCES a powerful tool for extending our knowledge of the low-mass regime of the initial mass function as well as star-formation in  $0.5 < z < 1$  galaxy clusters. We discuss design and fabrication issues and simulate the performance of the grism system.

**Keywords:** near-infrared, spectroscopy, grism

## 1. INTRODUCTION

Large format ( $1024^2/2048^2$  pixel) near-infrared detector arrays allow astronomers to map wide-angle structures and to survey broad areas of the sky with unprecedented sensitivity. With a large field-of-view, astronomers can avoid the photometric inaccuracies and operational overheads associated with mosaicing many smaller frames obtained over several nights, possibly under different sky conditions. Imaging and multi-object spectroscopy of star formation regions, stellar populations in external galaxies, galaxy clusters, and quasar environments are just a few examples of astronomical observations that profit from wide-field instruments.

During the last two years we have developed and used a new wide-field imager (PISCES) on the Steward Observatory 2.3m telescope. To date, PISCES has proven very popular in a wide variety of scientific applications, including identifying low-mass stars and brown dwarfs in young stellar clusters, studying the large-scale environments of quasars, and measuring star-formation of  $0.5 < z < 1$  galaxy clusters. It will be especially powerful at the 6.5m MMT and Magellan telescopes. In this paper we describe our plans to equip PISCES with a multi-object grism system for low-resolution spectroscopy.

## 2. PISCES: A WIDE-FIELD, 1-2.5 $\mu$ m IMAGER

PISCES<sup>1</sup> was conceived as a low cost (\$12k) instrument to utilize and optimize the HAWAII detector which was purchased for ultimate use in the ARIES instrument.<sup>2</sup> The up-looking dewar, depicted in Figure 1, was available from the former FASTTRAC<sup>3</sup> tip/tilt instrument and was reconfigured slightly to accommodate the new optics. To conserve costs, the dewar modifications and optics were designed to allow a circular field-of-view within the  $1024^2$  detector format. With the exception of the dewar window, all optical elements are cooled to  $\leq 77$ K by either liquid or solid nitrogen.

PISCES incorporates refractive optics to reimagine the focal plane from telescopes with f-ratios as fast as f/9 onto a HAWAII ( $1024^2$  pixel) detector at f/3.3. The resulting fields-of-view on the 2.3m Bok reflector and 6.5m MMT are 8.5/3.1' diameter at plate scales of 0.5/0.18"/pixel, respectively. The optical design (Figure 1) incorporates six lenses with all-spherical surfaces. All lenses are anti-reflection coated for  $\geq 98\%$  transmission from 1-2.5  $\mu$ m. For details of the optical design, see McCarthy et al.<sup>1</sup>

Other author information:

R.A.F.: Email: rfinn@as.arizona.edu; Telephone: 520-621-6535; Fax: 520-621-1532

D.W.M.: Email: mccarthy@as.arizona.edu; Telephone: 520-621-4079; Fax: 520-621-1532

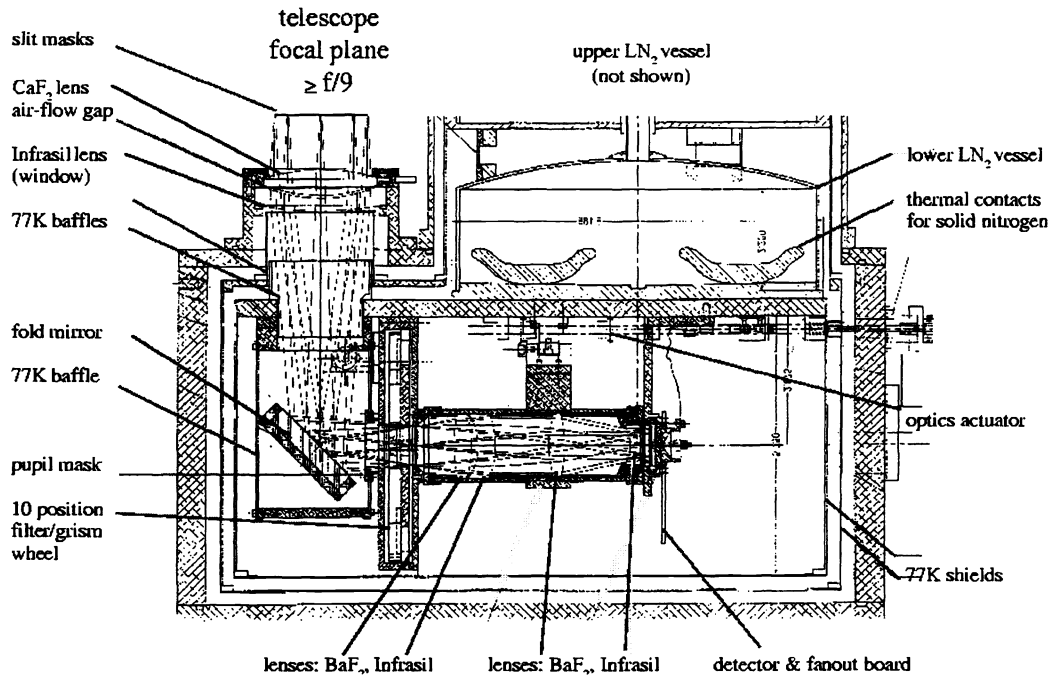


**Figure 1.** Schematic of the PISCES wide-field camera showing the optical configuration including the six refractive elements, filter wheel, pupil stop, and detector.

At the 2.3m Bok telescope at  $f/9$ , PISCES produces spot diameters (FWHM) of  $\leq 2$  pixels across the full  $8.5^\circ$  field in the standard J, H, K infrared photometric bands. Optical distortion is 3% at the field edge and can be completely corrected through standard image processing. Ghost images occur at the 0.3% level and are generally non-existent. We have measured a telescope emissivity of 5% and throughput (telescope + PISCES) of 50-55%. PISCES will operate at the  $f/9$  focus of the new 6.5m MMT without any modifications because its optical design was optimized for this  $f$ -ratio. In fact, the predicted spot sizes across the field are somewhat improved ( $\leq 1.5$  pixels) over those at the 2.3m telescope. Photometric sensitivities measured at the Bok 2.3m and predicted for the 6.5m MMT are listed in Table 1.

PISCES is well matched to the seeing conditions expected at the MMT. The best measure of these conditions comes from detailed analyses of image motion by our adaptive optics group using the old 4.5m MMT.<sup>4</sup> In contrast to the facility V+R-band measurements of FWHM, image motion samples the atmospheric and dome seeing components independently of the instrumental point-spread function. Typically, we have recorded a Fried parameter,  $r_0$ , of 0.9m at K-band with 2nd and 10th percentile values of approximately 3-4m and 2m, respectively. Extrapolating these values to H-band, we generally expect FWHM of  $0.53''$  with 10th percentile value of  $\sim 0.24''$ . Actual image quality may be even better due to new improvements in thermal management of the telescope optics and of the overall facility. Expected errors in telescope tracking ( $0.070''$ ) and anticipated wind-shake ( $0.05''$  for winds  $\leq 11\text{m/sec}$ ) should not degrade the above performance significantly. Based on the expected Fried parameter and on the discussion of Martin,<sup>5</sup> the tip/tilt component of atmospheric seeing should be  $0.15''$  (two-dimensional), the removal of which would yield only slight improvements in FWHM.

### 3. THE ADDITION OF GRISM SPECTROSCOPY

We plan to equip PISCES with a grism for low resolution ( $R=200-500$ ) single and multi-object spectroscopy. A spectral resolution of 500 affords reasonable resolution of OH lines while keeping the length of spectra short enough

**Table 1.** PISCES Camera Performance

	Measured at 2.3m Bok	Expected at 6.5m MMT
Field-of-view (diam.)	8.5 '	3.1 '
Scale	0.5 "/pixel	0.18 "/pixel
Optical spot (diam.)	<1.5 pixels	< 1.5 pixels
Median seeing (H-band)	1.2" FWHM	0.53" FWHM
Throughput	50-55%	50-55%
Emissivity	5-7%	5-7%
Limiting mag ( $10\sigma$ /min)	J 17.5 mag H 17.0 K <sub>s</sub> 16.5	J 20.5 H 19.4 K <sub>s</sub> 18.2

(240 pixels) to capitalize on multi-object capability. This resolution is important for studying star-formation in  $0.5 < z < 1$  galaxy clusters, as described in Section 3.3. At the MMT, this resolution requires a slit width of  $0.36''$ . In poorer seeing conditions, lower spectral resolution ( $R \sim 200-300$ ) can be achieved by widening the slits. Lower resolution is useful for classifying red dwarf stars and substellar objects as well as for understanding the surface chemistries of Kuiper Belt Objects. At the 2.3m telescope, with a pixel scale of  $0.5''/\text{pixel}$ , the one arcsecond wide slits required to preserve the grism resolution are well-matched to the typical seeing at the site.

### 3.1. Grism Design

The grism will be placed immediately behind the cold pupil stop (see Figure 1), and order-sorting filters will be placed in the existing 10-position filter wheel. Since the grism will be in a diverging beam, a small wedge angle is desired to minimize the aberrations introduced by placing a dispersive element in a diverging beam. Therefore, we prefer to make the grism from a high index material. Unfortunately, high index materials do not match the indices of replicating epoxies, and direct ruling of grisms is more expensive. We are currently investigating three options that differ from conventional grism fabrication methods.

The first optical design employs a Zinc Selenide (ZnSe) - Calcium Fluoride (CaF<sub>2</sub>) grism (Figure 2). A wedge angle of 6.9 degrees and groove spacing of 32 lines/mm allow J, H, and K-band spectroscopy in orders 5, 4 and 3, respectively. We have split the grism into a ZnSe prism and CaF<sub>2</sub> grating to circumvent manufacturing problems associated with ZnSe while still benefitting from a small wedge-angle afforded by ZnSe's high refractive index. Because ZnSe is brittle, ruling a diffraction grating directly onto the prism has produced grisms with low efficiency (20%<sup>6</sup>). Replicating a grating onto a ZnSe prism is not desirable since we do not know of an epoxy with matching index of refraction. Unlike ZnSe, CaF<sub>2</sub> has a resin with a matching index of refraction so a grating can be replicated onto CaF<sub>2</sub>. All surfaces will have anti-reflection coating to improve transmission. We ray-traced the ZnSe+CaF<sub>2</sub> grism with ZEMAX, and the resulting spot diagrams expected at the 6.5m MMT are shown in Figure 3. At the 2.3 and 6.5m telescopes, this design produces Nyquist sampled spectra of resolution 500 across 90% of the field; the resolution degrades slightly at the edge of the field.

We are also exploring the possibility of using a silicon grism and are collaborating with Dr. J. Ge at Pennsylvania State University. Dr. Ge and colleagues at LLNL<sup>7,8</sup> have recently manufactured silicon grisms using an etching technique and have implemented them for use in astronomy. The use of silicon permits a smaller wedge angle and, in principle, can yield better image quality in our slightly diverging beam. Unfortunately, the transmission of silicon cuts off shortwards of 1.2 microns, compromising spectral coverage in the J-band.

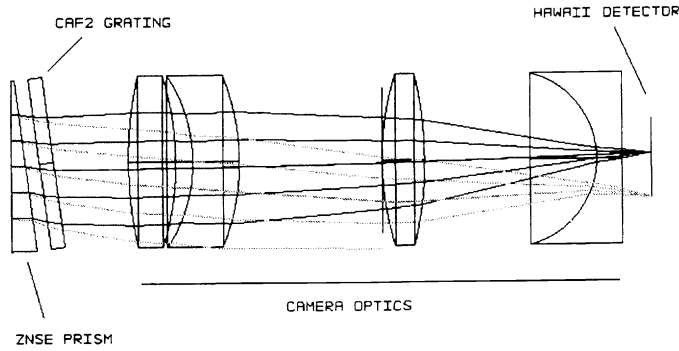


**Figure 2.** Raytrace of ZnSe + CaF<sub>2</sub> grism for center and edge-of-field rays. The grism is located just behind the cold pupil stop, and order-blocking filters can be placed in an already-existing filter wheel at the pupil. Edge-of-field rays will suffer slight vignetting. The grism will produce R = 500, Nyquist sampled spectra over 90% of the field.

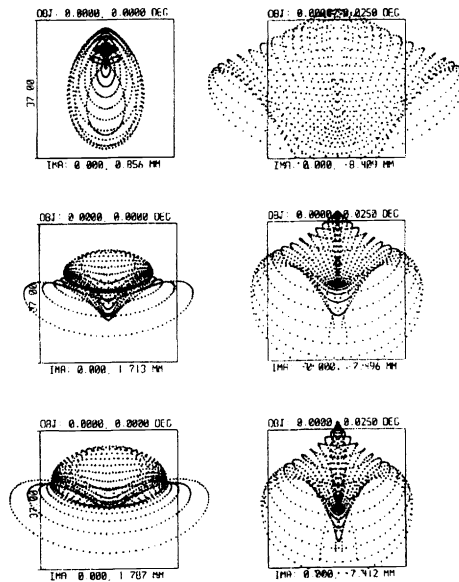


**Figure 3.** Expected spot-sizes (top to bottom) at 1.25 $\mu$ m, 1.65 $\mu$ m, and 2.2 $\mu$ m for a simulated ZnSe + CaF<sub>2</sub> grism used in PISCES on the 6.5m MMT. On-axis and edge-of-field spots (1.5') are shown in the left and right columns. Boxes correspond to a width of two pixels (37 $\mu$ m).

The final material being investigated for the grism is Arsenic Trisulfide. This material has a melting temperature of  $\sim 200$  C and can be molded directly onto a master grating. Researchers at Hyperfine, Inc. have made such devices. We are exploring the suitability of this material for cryogenic applications since its thermal conductivity is lower and thermal expansion higher than traditional materials. If the diffraction efficiency is comparable to replication, this may be our best option.

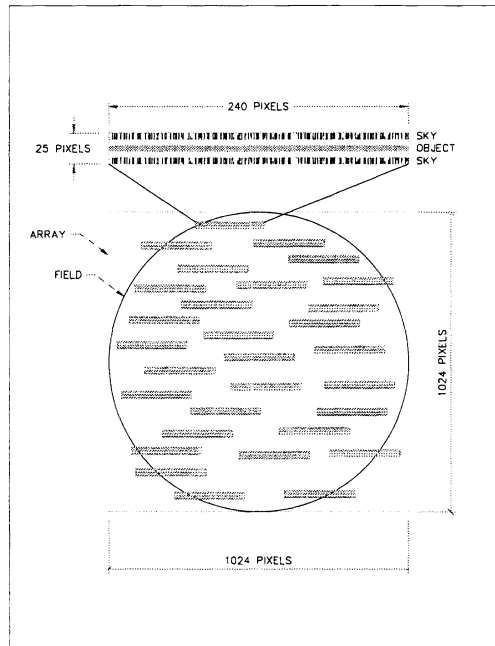


**Figure 4.** Example layout of 30 spectra on the HAWAII detector array in PISCES when used at the 6.5m MMT at  $f/9$  ( $0.18''/\text{pixel}$ ). Each spectrum is  $25 \times 240$  pixels. Although the field-of-view is a  $3.1'$  diameter circle, spectra can be recorded over the full detector array ( $1024^2$  pixels).

### 3.2. Slit Masks

A slit-mask with either single or multiple slits will be placed at the focal plane, 40mm above the entrance window to the dewar. On the MMT, the  $0.36''$  slits required for  $R = 500$  must be  $0.1\text{mm}$  wide. We are investigating two avenues for manufacturing such masks. The first method uses a photo-chemical process available at Microphoto, Inc. (Roseville, MI). This company manufactures the cold pupil masks used in PISCES to a tolerance of  $0.001$  inch. For a tooling and manufacturing cost of  $\$500$ , they will fabricate 20 different masks on a single sheet of thin gauge stainless steel. Microphoto can make and ship masks within a few days of receiving an order.

A second, more attractive method is to fabricate the slit-masks in-house using a Laser Micromachining facility in the Steward Observatory Radio Astronomy Laboratory. The laser micromachine is operated under the direction of Dr. Chris Walker. Using a target image created in Autocad, the laser micromachine can cut the  $0.1\text{mm}$  slits from a thin slab of silicon to an accuracy of  $3\mu\text{m}$  with an edge roughness of  $200\text{nm}$ . The slit-mask can then be coated with gold in the Steward Observatory CCD Laboratory to minimize emissivity. This method could reduce the fabrication time for the masks, and the primary costs would be for the silicon and gold. The laser micromachining system will be operational by the end of 2000.

The number of slits per mask will vary greatly from field to field. With an ideal arrangement of targets, we could obtain 40 spectra simultaneously. More realistic positioning of sources will permit 20-30 slits per mask. In a random field, 67% of the objects would have their full spectra contained on the detector array. Figure 4 shows how 30 spectra can easily fit on the array, even with slit-lengths of  $5''$  to allow adjacent sky spectra around each object. A mask will be fabricated for each field based on target lists and positions generated from previous PISCES images or other coordinate lists. We can adapt Dr. John Hill's fiber positioning software to maximize the number of slits per mask and to group targets with similar magnitudes.

Although the grism mentioned above is designed for J, H and K-band spectroscopy, thermal emission from the warm slit-mask will compromise sensitivity beyond  $1.6\mu\text{m}$ . This background might be reduced by several techniques, such as using low emissivity material or coatings on the masks and packaging the masks in a mini-dewar over the

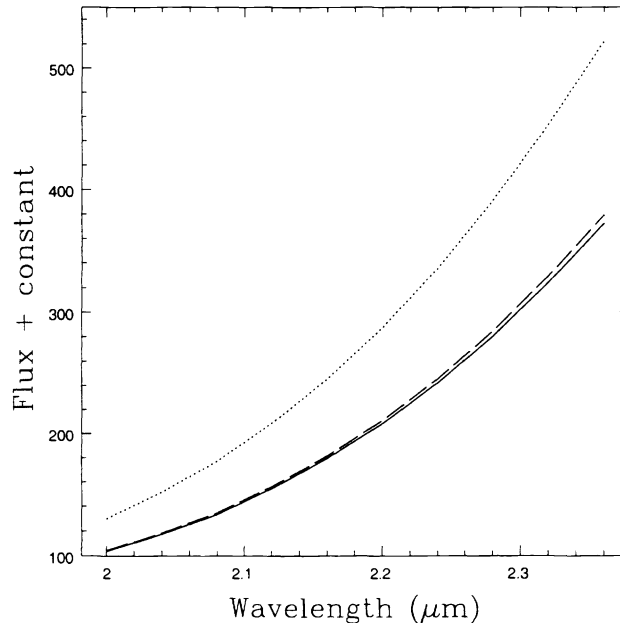


**Figure 5.** Comparison of K-band flux detection threshold for warm slit-masks (dotted), masks cooled 40 K below ambient with a thermo-electric cooler (dashed) and masks cooled to 77 K (solid). This assumes a slit-mask emissivity of 15%. Clearly, the greatest gain in sensitivity is achieved by the thermo-electric cooler.

main dewar window so they can be thermo-electrically cooled. Figure 5 shows a comparison of K-band sensitivity for warm slit-masks, thermo-electrically cooled slit-masks and liquid nitrogen cooled slit-masks. The largest gain in sensitivity (a factor of 1.4) is achieved when cooling the masks from ambient temperature to 40 K below ambient with a thermo-electric cooler. The slit-masks can be housed in a vacuum tight assembly that will attach around the entrance window of the dewar. With such a small enclosed volume, the slit-mask housing can be evacuated and cooled quickly, allowing for easy exchange of slit-masks during the night or over the course of an observing run.

### 3.3. Simulation of Grism Performance

PISCES' multi-object grism system is ideally suited to measure star-formation rates in  $0.5 < z < 1$  galaxy clusters. Currently, very few studies have been conducted to study the star-formation histories of galaxy clusters in this redshift interval, and no star-formation estimates have been made using  $H\alpha$ . Two reasons for this dearth of information are that spectroscopy takes a long time and  $H\alpha$  moves out of the visible window past  $z = 0.5$ . Equipped with a multi-object grism system, PISCES will enable interested astronomers to make some of the first star-formation measurements for high-redshift galaxy clusters, and the multi-object capability will ensure efficient use of telescope time.

We have simulated the performance of the PISCES grism system to predict its sensitivity for measuring star-formation rates for  $0.5 < z < 1$  galaxies. According to Coleman, Wu & Weedman,<sup>9</sup> the expected  $V$  magnitude of a  $z \approx 1$  spiral is 23 - 24. Poggianti<sup>10</sup> predicts the  $V - J$  color of a  $z \approx 1$  spiral to be 2.5 - 3 magnitudes. Thus, it's reasonable to assume a  $J$  magnitude of 21 for a  $z \approx 1$  spiral, and this is what we use to simulate the grism performance. In Figure 6, panel (a) shows the original galaxy spectrum of NGC 6127 used for this simulation. According to Kennicutt,<sup>11</sup> the equivalent width of the  $H\alpha + [NII]$  emission for this galaxy is  $40\text{\AA}$ . Kennicutt<sup>11</sup> also reports that normal galaxies have equivalent widths of  $H\alpha \leq 40\text{\AA}$ , so this galaxy is representative of a typical, star-forming galaxy. To simulate the performance of the grism, we first redshift the galaxy spectrum to  $z = 1$  and convolve with a gaussian so that the resultant spectrum has a resolution of 500. The flux of the galaxy is scaled to

correspond to  $J = 21$  for a 3-hour integration, as shown in panel (b). A resolution 500 night sky spectrum, scaled for a 3-hour integration and shown in panel (c), is then added to the galaxy spectrum. Poisson noise, detector read-noise and dark current are added to the sky+object spectrum, and a smoothed sky spectrum is subtracted. The resulting galaxy spectrum is shown in panel (d). The signal-to-noise per pixel of the  $H\alpha + [NII]$  emission feature at  $1.31\mu\text{m}$  averages around 20.

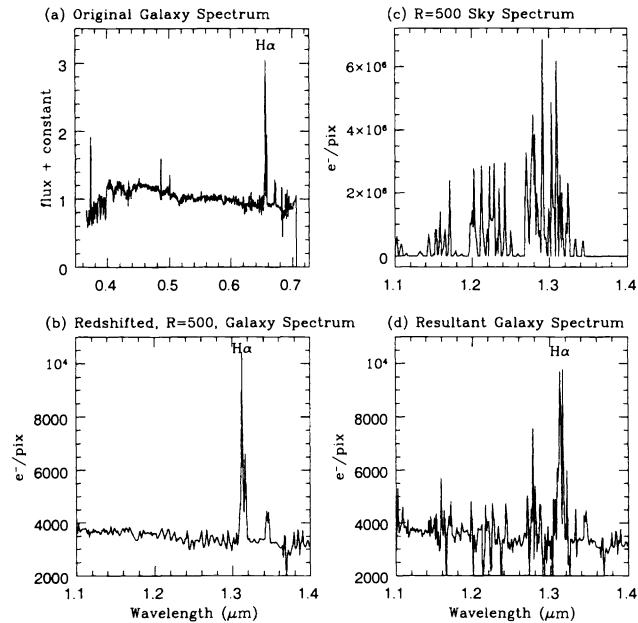


**Figure 6.** Simulation of grism’s sensitivity for measuring star-formation rates in  $z \leq 1$  galaxies. Panel (a) shows the visible spectrum of NGC 6240. In panel (b), the spectrum is redshifted to  $z = 1$  and convolved with a gaussian so the resulting resolution is 500. The galaxy spectrum is scaled to correspond to the flux of a  $J = 21$  galaxy after 3 hours of integration. Panel (c) shows a resolution 500 night-sky spectrum, also scaled for a 3-hour integration. After adding Poisson noise, readout noise and dark current to the sky + galaxy spectrum, a smoothed sky spectrum is subtracted to yield the spectrum in panel (d). The signal-to-noise per pixel of the redshifted  $H\alpha$  feature is  $\sim 20$ .

Star-formation measurements based on field galaxies<sup>12</sup> show a steady increase in star-formation rates versus redshift, at least out to  $z \approx 2$ . Therefore, it is not unreasonable to assume that galaxies in clusters will also have higher star-formation rates, and thus stronger  $H\alpha$  emission, at  $z \approx 1$ . A resolution 500 grism, in addition to wide-field multi-object capabilities, makes PISCES an ideal and uniquely suited instrument for studying the evolution of star-formation in galaxy clusters.

#### 4. SUMMARY

We have discussed plans to upgrade an already existing wide-field infrared camera with a multi-object grism system for use at the Steward 2.3m and 6.5m MMT. The design allows J, H, and K-band spectroscopy in orders 5, 4 and 3, respectively. The grism will be placed at the cold pupil, in a slightly diverging beam, and we are exploring three different materials for the grism that will allow for a small wedge angle, thereby minimizing the aberrations caused by placing a dispersive element in a diverging beam. Single or multi-object slit-masks will be placed at the focal plane, above the entrance to the dewar, and we have determined that a thermo-electric cooler is sufficient for minimizing thermal emission from the slits. The combination of 6.5m aperture and multi-object capability will make PISCES a powerful tool for extending our knowledge of the low-mass regime of the initial mass function as well as star-formation in  $0.5 < z < 1$  galaxy clusters. We hope to have the grism system operational by the end of 2000.

## REFERENCES

1. D. McCarthy, J. Ge, J. L. Hinz, R. A. Finn & R. S. deJong, "PISCES: A Wide Field, 1-2.5 $\mu$ m Camera For Large Aperture Telescopes", in preparation.
2. R. Sarlot, D. McCarthy, J. Burge & J. Ge, "Optical design of ARIES: The New Near Infrared Science Instrument for the Adaptive f/15 Multiple Mirror Telescope", *SPIE*, **3379**, in press.
3. L. Close & D. McCarthy, "High-resolution imaging with a tip-tilt Cassegrain secondary", *Publications of the Astronomical Society of the Pacific*, **106**, 77, 1994.
4. M. Lloyd-Hart et al., "First Astronomical Images Sharpened with Adaptive Optics using a Sodium Laser Guide Star", *Astrophysical Journal*, **493**, pp. 950-954, 1998.
5. H. M. Martin, "Image Motion as a Measure of Seeing Quality", *Publications of the Astronomical Society of the Pacific*, **99**, pp. 1360-1370, 1987.
6. J. T. Raynor, "Evaluation of a Solid KRS-5 Grism for Infrared Astronomy", *SPIE*, **3354**, pp. 289-294, 1998.
7. J. Ge, D. Ciarlo, P. Kuzmenko, B. Macintosh, C. Alcock, K. Cook, D. Gavel, C. Max, J. Lloyd, J. Graham, M. Liu & S. Sevenson, "The First Light of the World's First Silicon Grisms", American Astronomical Society Meeting 195, 87.15, 1999.
8. J. Ge, D. Ciarlo, P. Kuzmenko, C. Alcock, B. Macintosh, J. R. P. Angel, N. Woolf, M. Lloyd-Hart, R. Fugate & J. Najita, "Adaptive Optics High-Resolution Spectroscopy: Present Status and Future Direction", *SPIE*, **3762**, pp. 174-183, 1999.
9. G. D. Coleman, C.-C. Wu & D. W. Weedman, "Colors and Magnitudes Predicted for High Redshift Galaxies", *Astrophysical Journal Supplement Series*, **43**, pp. 393-416, 1980.
10. B. M. Poggianti, "K and Evolutionary Corrections from UV to IR", *Astronomy & Astrophysics*, **122**, pp. 399-407, 1997.
11. R. C. Kennicutt, Jr., "The Integrated Spectra of Nearby Galaxies - General Properties and Emission-Line Spectra", *Astrophysical Journal*, **388**, pp. 310-327, 1992.
12. P. Madau, L. Pozzetti & M. Dickinson, "The Star Formation History of Field Galaxies", *Astrophysical Journal*, **498**, pp. 106 - 116, 1998.